Transient Thermal Analysis of Screw Compressors

Part II – Application

J. Sauls, **G. Powell**, **B. Weathers,** Trane, La Crosse/USA

Abstract

This is the second of a two-part report on the transient thermal analysis of screw compressors. This work was undertaken to better understand rotor-to-housing and rotor-to-rotor clearances. Reliability and performance are functional characteristics of the compressor that are strongly dependent on the operating clearances. It is important that these be understood in the context of operation under the influence of pressure and thermal loads. Development of the analysis process is described in Part I of this report; application of the methods and some experimental results are presented here.

Introduction

Part I of this report described adaptation of an analytical process defined in [1] to use in transient analysis of refrigerant screw compressors. In this part, results of application of the analyses are reviewed. First, computed temperature characteristics at selected points on the compressor housings and rotors are compared to transient experimental results. Following this, predicted rotor-to-housing and rotor-to-rotor clearances are presented.

Calculation of Metal Temperatures

The analysis described in Part I was applied to a screw compressor designed for operation with refrigerant R134a and used in air-cooled water chillers. A transient analysis for a compressor start are carried out. In this case, the initial state of the parts is a uniform temperature of 20°C, typical ambient conditions. The compressor starts with the mechanical unloading devices set for operation at minimum capacity. For a typical water chiller application the unit will reach a steady-state operating condition where the compressor inlet saturation temperature is 4.8°C and the discharge saturation temperature is 22.2°C. This operating condition imposes a relatively low 1.8 pressure ratio on the compressor. A compressor was run on a test stand from a cold, stabilized state with the compressor off to steady-state operation at the 1.8 pressure ratio condition. Inlet and discharge pressures were recorded during the transient operation.

The operating history, defined by operating conditions vs. time, was divided into eleven time steps to define the transient path for analysis. At the end of each time step, the measured operating conditions were input into the thermodynamic simulation program. As explained in Part I, this provides estimates of fluid temperatures and heat transfer coefficients at the fluid-solid boundaries which are transferred to the finite element model as boundary conditions. The finite element model was run from the cold, off state through the first time step. This solution became the initial condition for the next step. Boundary conditions were updated to those computed at the end of the second time step and the finite element solution was run again. This process was repeated 11 times to arrive at the analytical estimate of rotor and housing temperatures during this start-up transient.

Figure 1 shows the computed boundary conditions mapped onto the housing and rotor surfaces at one of the time steps. For clarity, only the boundary conditions for surfaces within the compression section are shown. Fluid temperature and heat transfer coefficient are defined for all model surfaces in the analysis.

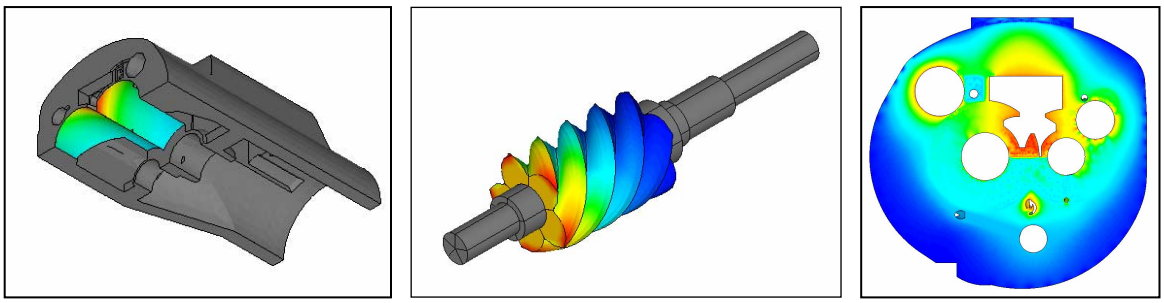

(a) (b) (c)

Fig. 1: Boundary conditions mapped onto compressor surfaces

Figure 1a shows the interior surface if the main housing with the heat transfer coefficient levels indicated in the contours, red being high levels, blue the low levels. Fluid temperature boundary conditions at the part surfaces are shown in Figures 1b and 1c for the male rotor and the discharge end bearing housing, respectively.

Figure 2 shows external housing temperatures computed at two different time steps in the transient run. Figure 2a is at a time shortly after the start of the solution. The dark blue represents temperatures around the initial state of 20°C. As we can see, the area around the compressor discharge port to the left on the figure is just beginning to show higher temperatures. Figure 2b shows the housing much later in the process. In this case, the temperatures are approaching, but have not yet reached, the steady-state condition.

In addition to solving the heat transfer problem to get estimates of part temperatures, the deformations of rotors and housing parts are computed at each time step. This information is then processed to provide estimates of rotor-to-housing and rotor-to-rotor clearances.

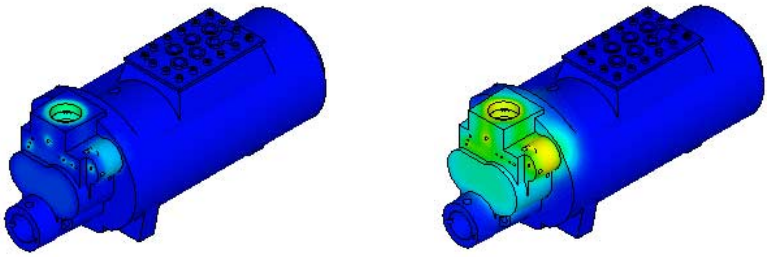

(a) (b)

Fig. 2: Compressor housing external temperatures during transient operation

Comparison of Calculated and Measured Metal Temperatures

Assessment of the model's capabilities is made by comparing the computed transient temperature characteristics to measurements taken on the compressor run through the transient tests. The compressor was instrumented with 30 thermocouples, 6 on each rotor, 10 on the discharge end bearing housing and 8 on the main rotor housing.

The approximate locations of 9 of the thermocouples on the rotor and bearing housings are shown in Figure 3 by the small round symbols. The figure is a horizontal section through the compressor, with the high pressure side of the rotor bores, the discharge port and the discharge end bearing cavities visible. The thermocouples are not on the surfaces, but in the metal at various depths away from the fluid-solid interface.

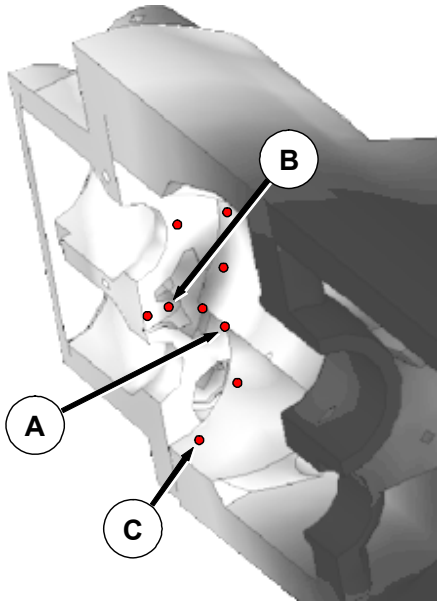

Fig. 3: Housing instrumentation

Following is a comparison of the measured and computed temperature vs. time characteristics at the locations labeled A, B and C in the figure. Figure 4 shows the comparison for location A. This is a point near the cusp, the intersection of the male and female rotor bores, at the discharge end of the compressor, not far from the radial discharge port. It is here that the highest metal temperatures are calculated.

We can see in the figure that the calculations compare very favorably to the measured results. The rate of temperature rise in the early part of the process is modeled well, as are the point of maximum temperature and the subsequent slow drop as operation approaches steady-state.

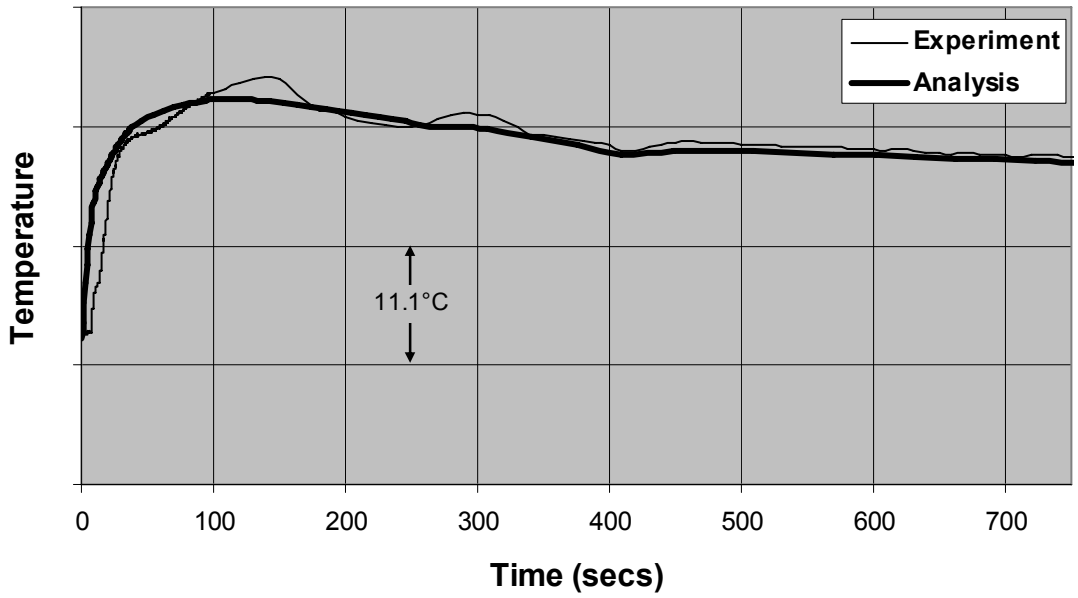

Fig. 4: Comparison of calculated and measured transient temperatures at location A

The comparison of measured and computed temperatures at location B is shown in Figure 5. This measurement point is on the bearing housing at the discharge port. The comparison

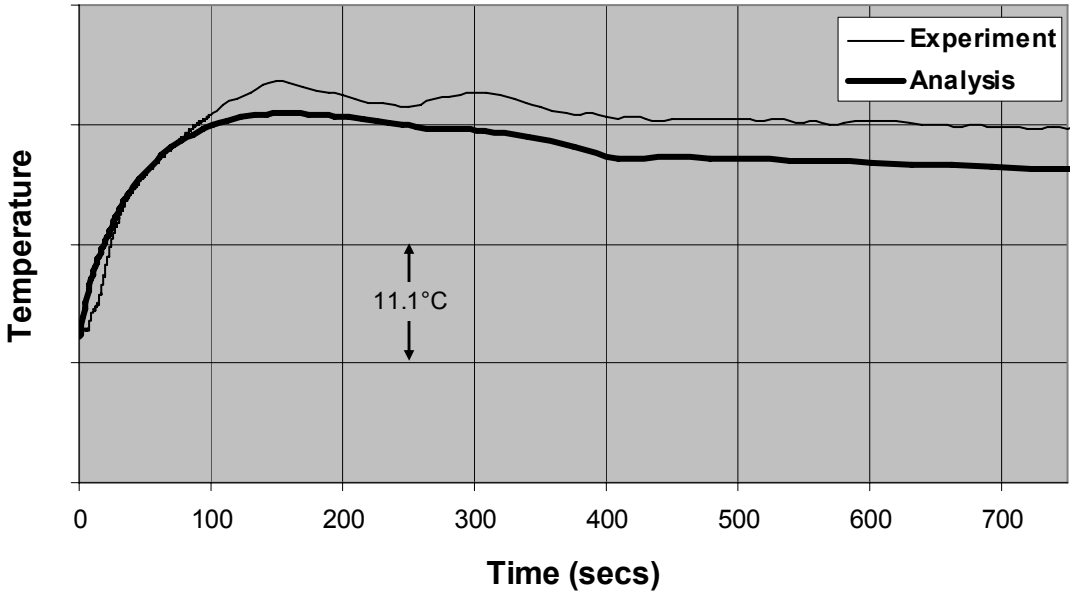

Fig. 5: Comparison of calculated and measured transient temperatures at location B

between the measured and computed results is not as good as for location A, but characteristics such as the initial rate of change in temperature and the time at which the temperature reaches a maximum are still fairly well represented by the model. Approaching the stead-state condition, the model under-predicts the temperature by about 5°C.

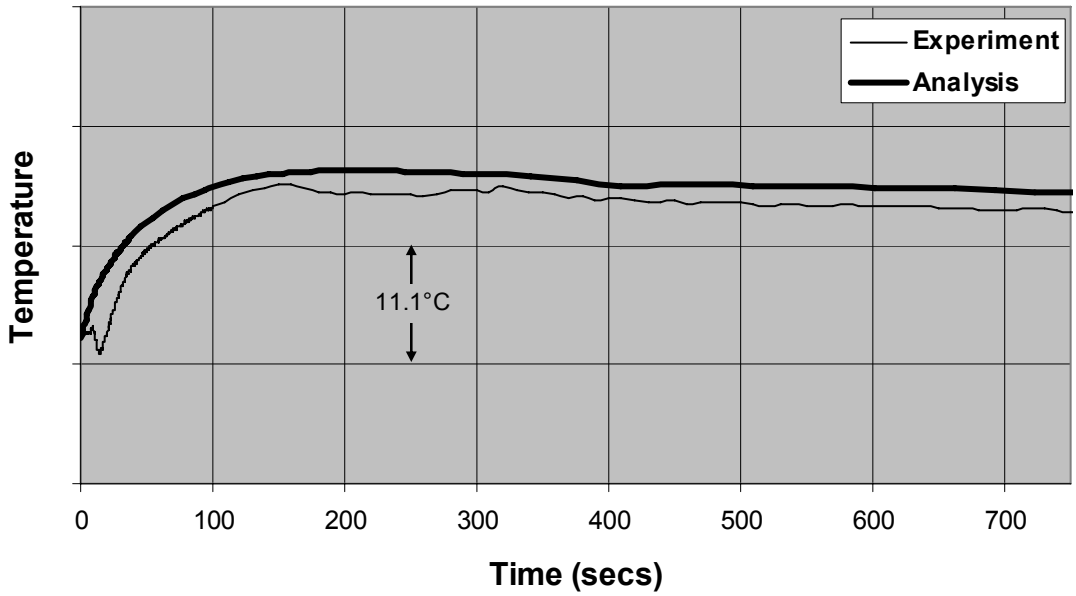

Fig. 6: Comparison of calculated and measured transient temperatures at location C

Figure 6 shows the final comparison between measured and computed housing temperatures. Location C (Figure 3) is on the female rotor side rotor bore, near the discharge end of the compressor. Once again, the agreement between measurement and calculation is relatively good. The characteristics of the measured temperature in the first 20 seconds are not seen in the analysis. However, the rate of change of temperature after this time and the point of temperature maximum are will predicted.

Further discussion of housing temperature calculations and clearance computations can be found in reference [2].

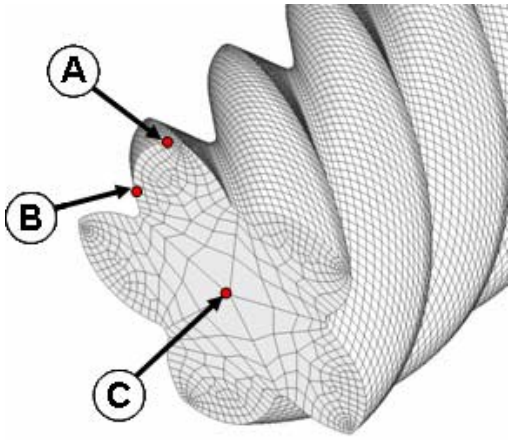

Fig 7: Male rotor measurement locations

Thermocouples are also installed on the male and female rotors, with the signal output delivered via slip rings on the shaft ends. On each rotor there is a measurement point near the lobe tip, location A in Figure 7, which shows the male rotor. The second location is near the rotor drive

band, location B, and a third at the rotor centerline, location C. Corresponding points are measured on the female rotor. These locations are measured at planes near the compressor discharge and midway between the discharge and inlet ends. Comparison of measured and computed temperatures is shown in Figure 8. Comparisons at locations A, B and C (Figure 7) are in the top, middle and bottom charts, respectively, in the figure.

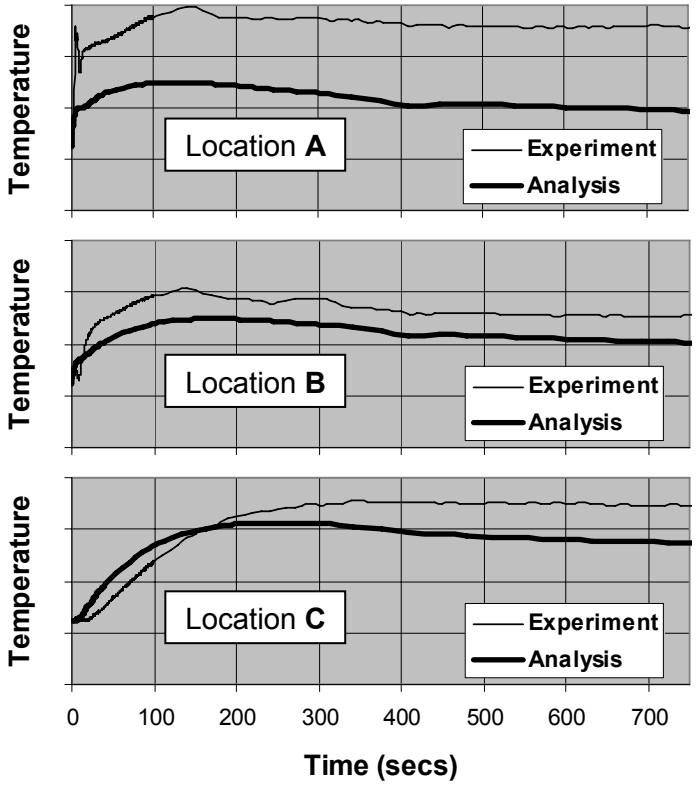

Fig 8: Comparison of calculated and measured transient male rotor temperatures at the discharge end

Agreement between measured and computed clearances is not as good for the rotors as it was for the housings. This is especially true for the rotor tip, location A with measured temperature levels being 10° to 15°C higher than the calculated temperatures. For locations B and C, rates of change of temperature and location of the temperature maximums are fairly well estimated.

Agreement between measurement and computation is much better at the plane in the middle of the male rotor and is also better for all female rotor measurement locations. Figure 9 is a comparison at the female rotor tip, discharge end.

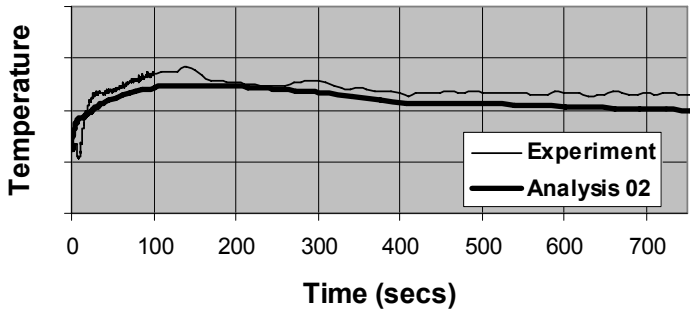

Fig 9: Comparison of calculated and measured transient female rotor temperatures at the discharge end

Considering the simplicity of the models relative to the complex phenomena occurring in the compressor, we consider the agreement between calculated and measured temperatures to be quite good.

Calculation of Transient Rotor-to-Housing Clearances

The next step in the analysis is to use the computed temperature characteristics to compute the transient clearance characteristics. Results of the computation of clearance between the male rotor and the main rotor housing bore are shown in Figure 10.

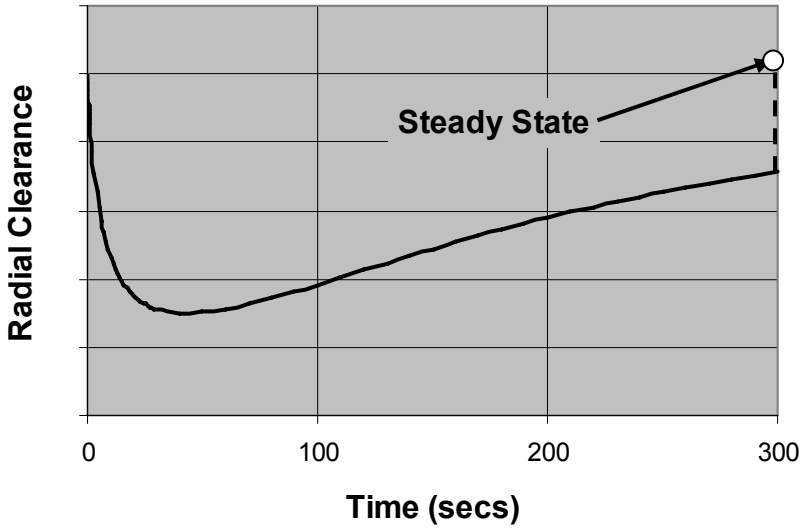

Fig. 10: Computed male rotor side rotor-to-bore transient clearance characteristic

The point at which the clearance is evaluated is very near the measurement location A, shown in Figure 3. The analysis reveals two important characteristics of the rotor-to-housing clearance. First, the steady-state operating clearance is virtually identical to the cold, as-built clearance. However, during the transient from the cold, as-built state to the loaded operating state, the clearance goes through a significant transient. There is an initial loss of clearance, occurring early in the process. This is followed by a more gradual increase in clearance back to the as-built levels. This is caused by the relatively large difference in the housing and rotor thermal inertias. Rotors, being less massive, tend to grow quickly while the heavier iron housing grows at a slower rate. The result is the initial loss in clearance shown in the figure.

Calculation of Steady-State Rotor-to-Rotor Clearances

Rotor-to-rotor clearances are analyzed at the steady state operating state. The calculated meshline clearance is shown Figure 11. The baseline, as-built clearance characteristic is shown along with the clearances computed during steady-state operation. Clearances are plotted along the three dimensional meshline. The x-axis scale is the fraction of the three-dimensional meshline length and runs from the inlet end of the rotor (position = 0.0) to the discharge end (position = 1.0). The area under this curve will then be proportional to the total leakage flow area of the full three-dimensional meshline. This method of presenting meshline

clearances and a more complete study of the rotor-to-rotor clearances may be found in reference [3]. Clearances are computed using a program that carries out a three-dimensional analysis of the rotor pair after the methods described in [4].

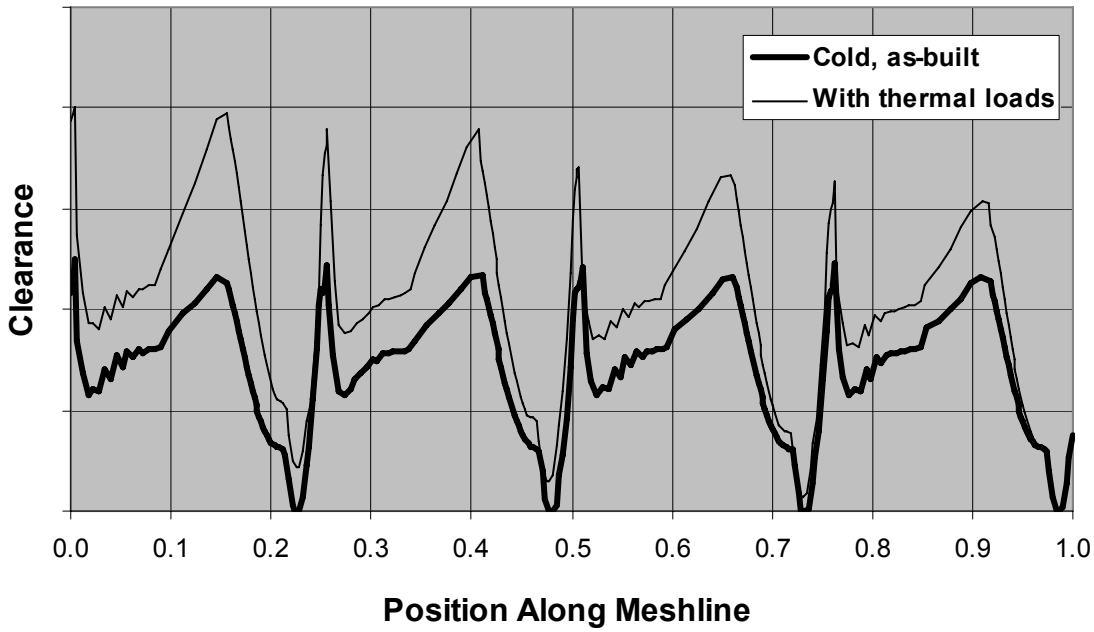

Fig. 11: Computed rotor-to-rotor steady-state clearance distribution

The computations carried out to generate the comparison shown in the figure include thermal effects on the shapes of the male and female rotor profiles and the effects of changing the orientation of the rotor shafts due to movement of the bearings. Effects of thermal loads on the relative locations of the bearing mounting planes are computed in the finite element model of the housings.

The combined effect of thermal deformation of rotors and housings is to increase the total intermesh leakage area and to change the rotor-to-rotor contact pattern; in this case, the leakage area increases by about 40%.

Figure 11 shows the clearances for only one rotor orientation. At this particular point in time, the rotor drive band has contact (zero clearance) only near the discharge end whereas for the aligned, un-deformed case, there are four contact locations along the meshline. As the rotors rotate, the minimum clearance points move along the x-axis, but in all cases, it is only in the region nearer the discharge end where we actually find contact in the drive band section of the profile.

Summary

Application of the analysis process described in Part I of this report reveals several important aspects of screw compressor clearance characteristics. For the rotor-to-housing clearances, the analysis shows that, for the particular design analyzed, clearances during steady-state operation are nearly identical to the clearances found in the cold, as-built state. However, a significant change in clearance is seen when the transient clearances are computed. This means it is necessary to understand transient operation in order to set target clearances for the design. Being able to analyze the transient case also provides the opportunity to design the parts to reduce the clearance excursions, allowing the nominal (and steady-state operational) clearances to be set to lower values, a performance benefit.

Rotor-to-rotor clearance in steady-state operation is increased relative to the steady-state condition according to the analysis. The rotors increase in size at the higher operating temperatures, tending to reduce clearance. However, the deformation in the housings at the bearing mounting points more than offsets this effect; hence, the net increase in clearance. The analysis also shows that the rotor-to-rotor contact characteristics are affected by the thermal loads. During operation at load, the contact band is located on the profile in the desired positions and is of about the correct size. This is seen in the agreement in the shape of the operating clearances in the vicinity of the zero-clearance region of the cold case.

Having an analysis such as the one described here provides opportunities for the compressor designer. Knowing the differences between transient and steady-state minimum clearance conditions allows for selection of nominal part dimensions that are more likely to provide expected results in terms of performance and reliability. The analysis also allows identification of the features or characteristics of the assembly that contribute to any undesirable conditions. Design alternatives can then be studied quickly and at very low cost.

Acknowledgements

My thanks Trane for the opportunity to present the work reported here. And my thanks to Prof. Dr.-Ing. Knut Kauder, Dipl.-Ing. Magnus Janicki and Dr.-Ing. Thomas von Unwerth for their invaluable advice. And thanks to my co-authors and colleagues. Bob Weathers is responsible for creation of the finite element models, execution of the analyses and examination of the rotor-to-housing clearances. Gordon Powell has implemented the rotor clearance calculation model and processed the thermal deformation results to arrive at rotor-to-rotor clearances.

References

[1] Kauder, K. and Keller, G., 1995, Wärmeübergangsrandbedingunen für Schraubenmaschinen, Schraubenmaschinen – Forschungsberichte des FG Fluidenergiemaschinen Nr. 13, Universität Dortmund: 5-19.

[2] Weathers, B., Sauls, J. and Powell, G., 2006, Transient Thermal Analysis of Screw Compressors, Part II Transient Thermal Analysis of a Screw Compressor to Determine Rotor-to-Housing Clearances, Accepted for publication in the Proceedings of the 18th International Compressor Engineering Conference, Purdue University.

[3] Powell, G., Weathers, B. and Sauls, J. 2006, Transient Thermal Analysis of Screw Compressors, Part III Transient Thermal Analysis of a Screw Compressor to Determine Rotor-to-Rotor Clearances, Accepted for publication in the Proceedings of the 18th International Compressor Engineering Conference, Purdue University.

[4] Janicki, M., 1996, Ein Programm zur Profileingriffsspaltberechnung von verformten Schraubenmaschinen, Schraubenmaschinen – Forschungsberichte des FG Fluidenergiemaschinen Nr. 13, Universität Dortmund: 108-112.